Delft University of Technology

Objective Inceptor Cueing Test for Control Loading Systems
Principle and Initial Design

Fu, Wei; van Paassen, Rene; Stroosma, Olaf; Mulder, Max

Important note
To cite this publication, please use the final published version (if applicable).
Please check the document version above.

Objective Inceptor Cueing Test for Control Loading Systems: Principle and Initial Design

W. Fu[*] , M. M. van Paassen [†] , O. Stroosma [‡] and M. Mulder[§]

Delft University of Technology, Delft, The Netherlands

Control loading devices are currently certified on the basis of tests on their mechanical properties, the criteria for these properties are not related to humans' ability to discriminate these properties. We propose the Objective Inceptor Cueing Test, a new design for control loading device evaluation based on humans' haptic percept limits (the Just Noticeable Difference (JND)). To this end we quantify the JND as a frequency response function (FRF). We consider the system to be excited by a sinusoidal motion input. A manipulator's FRF at the frequency of excitation can be considered as a complex-valued number, and JNDs respectively in its magnitude, phase angle, real and imaginary parts were obtained from seven human subjects. A model published previously was extended with these results to formulate an OICT perceptual fidelity region. With an admittance control protocol, our control loading device could be evaluated by the fidelity region formulation independently of the reference manipulator dynamics. Results showed that the device could preserve the original haptic perception of any stability-allowable manipulator dynamics up to 11 rad/s.

I.   Introduction

Flight simulators are nowadays widely used for pilot training and the relevant research. The Control Loading System (CLS) driving the simulator's control inceptor, aims to provide the pilot trainees with the force feel of the flight controls as they would have experienced in the real vehicle. The dynamics of the CLS consists of two parts: the desired manipulator dynamics and the servo system. The desired dynamics are generally defined by the motion-force dynamics of a manipulator. The device is typically configured as either an admittance or an impedance display.[1] The desired force or motion in response to measurements of the motion or force that pilots apply on the control inceptor is calculated in the control loading computer. The servo system is then fed by the desired kinetic information to move the inceptor in the desired way.

Due to dynamics of the servo system and the time delay caused by the discrete computation, an inevitable difference exists between the intended simulated manipulator dynamics and the dynamics actually realized. To ensure the fidelity of simulation, certifying standards are regulated by authorities. A common one is the EASA regulation[2] that involves a full range sweep and a free release measurements. Regular tests are required on control loading devices to maintain the original feel of control.

These requirements consider the control device in isolation, while the tactile feel is most relevant when the pilot is actually touching the manipulator. Since these evaluations overlook the preservation of the original haptic perception from the view of pilots, these time-domain measurements do not necessarily ensure a perfect "feel" reproduction. We intend to design an alternative criterion based on perceptual limits in terms of haptics. We propose to use data on the accuracy with which human operators can perceive the dynamics of a control inceptor, specifically the Just Notable Differences (JND) in a manipulator's dynamics. We label this the Objective Inceptor Cueing Test (OICT). Naming and philosophy of the test follow the work

---

[*]PhD Candidate, Section of Control and Simulation, Faculty of Aerospace Engineering, P.O. Box 5058, 2600 GB Delft, The Netherlands, w.fu-1@tudelft.nl.

[†]Associate Professor, Section of Control and Simulation, Faculty of Aerospace Engineering, P.O. Box 5058, 2600 GB Delft, The Netherlands, m.m.vanpaassen@tudelft.nl, Member AIAA

[‡]Researcher, Section of Control and Simulation, Faculty of Aerospace Engineering, P.O. Box 5058, 2600 GB Delft, The Netherlands, o.stroosma@tudelft.nl, Senior Member AIAA

[§]Professor, Section of Control and Simulation, Faculty of Aerospace Engineering, P.O. Box 5058, 2600 GB Delft, The Netherlands, m.mulder@tudelft.nl. Associate Fellow AIAA

American Institute of Aeronautics and Astronautics

on simulator motion system qualification and the Objective Motion Cueing Test.[3] In our view, such a psychophysical evaluation could give better guidelines.

In a control task, the position of the manipulator is determined by the requirements of the task, the resulting force is then a source of information for the human controller.[4] This makes a motion to force causality appropriate to define the dynamics from humans perspective, and a perceptual difference should originate from the perceived difference of the output (the force). Humans' difference threshold for the force is a constant fraction of the force intensity, which is characterized by the Weber's law.[5–8] Evaluation of the CLS could be performed in the time domain by looking at the force measurements. For instance take measurements of the force responses to a given motion of both reference and simulated devices, and check if any difference between corresponding samples exceeds the respective force difference threshold (a fraction of the amplitude of the corresponding sample). But this approach suffers from numerical problems when the value of a force sample is close to zero. In addition, validations upon limited number of motion types or conditions can not ensure the validation for all scenarios. To circumvent these problems we define the force difference as a change in the frequency response function (FRF) of the system. Consider a simple linear case, where the dynamics of a manipulator is described by a differential equation:

$$H(\omega) = \frac{F}{X} = a_0 + a_1 \cdot (j\omega) + a_2 \cdot (j\omega)^2 + ... + a_n \cdot (j\omega)^n \tag{1}$$

Where F denotes the force at grip, and X denotes the angular displacement of the manipulator. This transfer function uses $j\omega$ instead of the Laplace variable s to express the stationary response of the system. We use a higher order system rather than the commonly used second-order mass-spring-damper system, to include cases where multiple masses exist in the mechanical system.

Evaluation can be performed by looking at the difference between frequency responses of the simulated and reference manipulator dynamics. A boundary which is determined by the JND is required to estimate if a difference is perceivable. In this work, we define the area within this boundary as the perceptual fidelity region. Since a system's frequency response as a function of frequency is different at different frequencies, the size of the fidelity region may be affected. Thus the characterization for individual frequencies is necessary. In this study, we conducted our investigation at a single frequency, representative of frequencies utilized by participants when a motion profile can be freely chosen, in this case 6 rad/s. In order to excite the manipulator exactly at this frequency, subjects were asked to apply a sine angular displacement $x = 0.37 \cdot sin(6t)$ to the manipulator with the assist from a display. The frequency response at a specific frequency can be expressed as a complex number, we measured the size of the JND in terms of changes in its magnitude, phase angle, real and imaginary parts. The JNDs were measured by a forced-choice staircase procedure. We extended a model concluded by our previous work by the experimental results, and formulated the frequency-domain fidelity region as a function of the magnitude of the system's frequency response. Our control loading device was then evaluated by the fidelity region as an example of the OICT.

This paper is organized as follows: In the following section, the JND is analyzed in the frequency domain with the assist from a Nyquist plot. An JND model driven by our previous work is elaborated. In Section III we shall describe the experiment procedure and conditions. The experimental results are given in Section IV. The formulation of the perceptual fidelity region and the initial design of the Objective Inceptor Cueing Test will be included in Section V. An example of implementing the OICT is shown in Section VI. Contributions of this study are concluded in the last section.

II.   Frequency domain analysis

At a specific frequency, the system's frequency response is represented by a complex-valued number. By defining the real and imaginary components of this complex number as P_{re} and P_{im}, we can describe the system in polar coordinates:

$$\begin{aligned} |H(\omega)| &= \sqrt{|P_{re}|^2 + |P_{im}|^2} \\ \angle H(\omega) &= tan^{-1}(\frac{P_{im}}{P_{re}}) \end{aligned} \tag{2}$$

This system can be visualized on a Nyquist plot, for example the blue line in Fig. 1. Assume that the control loading system simulates such dynamics with a different frequency response, on the Nyquist shown as a vector with different magnitude and phase angle (for example the red dash line in Fig. 1). The difference

American Institute of Aeronautics and Astronautics
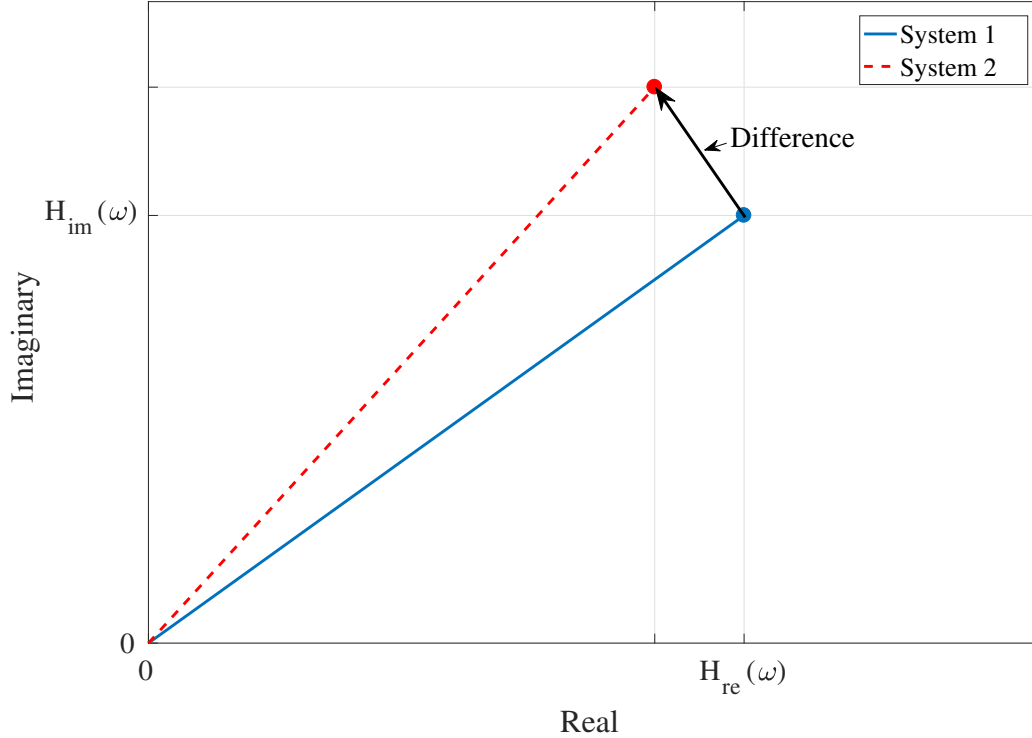
Figure 1: Nyquist plot of systems' frequency response at a specific frequency.

between the two systems' frequency responses, which determines the difference in their force responses to a sinusoid motion at this frequency, can also be described by a complex number:

$$\Delta H(\omega) = H_2(\omega) - H_1(\omega) \tag{3}$$

This difference vector is shown as the arrow in Fig. 1. The direction (phase angle) of this vector can be arbitrary, determined by the dynamics of the two systems. Our previous work[9] investigated the JND in terms of changes in the imaginary component of mass-spring-damper systems (changes caused by damping changes). In that case the difference vector is vertical. The size of such JND for a specific frequency normalized to the magnitude of the system's frequency response (the magnitude of the complex number) was found to be constant. This conclusion could be applied to systems with higher order as well, since the stationary force response of a system to a given motion is only determined by its magnitude and phase characteristics. At a specific frequency, as long as the FRFs of systems with different orders can be expressed by a same complex vector, JNDs in them should be identical.

Formulating the fidelity region involves quantifying the JND for dynamic changes pointing to all directions. We wonder if the magnitude of the system's frequency could be used to quantify the JND not only for the vertical difference but also for differences with other directions. Therefore we investigated JNDs in terms of several representative directions, respectively in the phase angle $\angle H(\omega)$, magnitude $|H(\omega)|$ and the real part $P_{re}(\omega)$. The JND for vertical changes (change in the imaginary part $P_{im}(\omega)$) was also tested to be used as the reference. Thus four conditions will be tested, and will be further elaborated in Section III. In this study, we consider the manipulator dynamics as a mass-spring-damper system, since such a system is representative of common control devices and easy to be programmed, and the frequency of excitation is 6 rad/s as discussed in the first section.

American Institute of Aeronautics and Astronautics

Table 1: Reference System Setting

Stiffness k	Mass m	Damping b
(Nm/rad)	$(Nm \cdot s^2/rad$ or $kg \cdot m^2)$	$(Nm \cdot s/rad)$
1.86	0.01	0.25

III.   Experiment Design

III.A.   Apparatus and participants

The experiment was performed in the Human-Machine Interaction Laboratory at the faculty of Aerospace Engineering, TU Delft. An electro-hydraulic side-stick manipulator was used to simulate the desired manipulator dynamics in the roll axis (left/right), which was fixed on the pitch axis. The griping point on the manipulator was 0.09 m above the rotation origin. An LCD screen, located in front of participants, was used to provide the reference side-stick angular displacement and the timing of experimental runs. An illustration of the devices can be seen in Fig. 2.

(a)   (b)
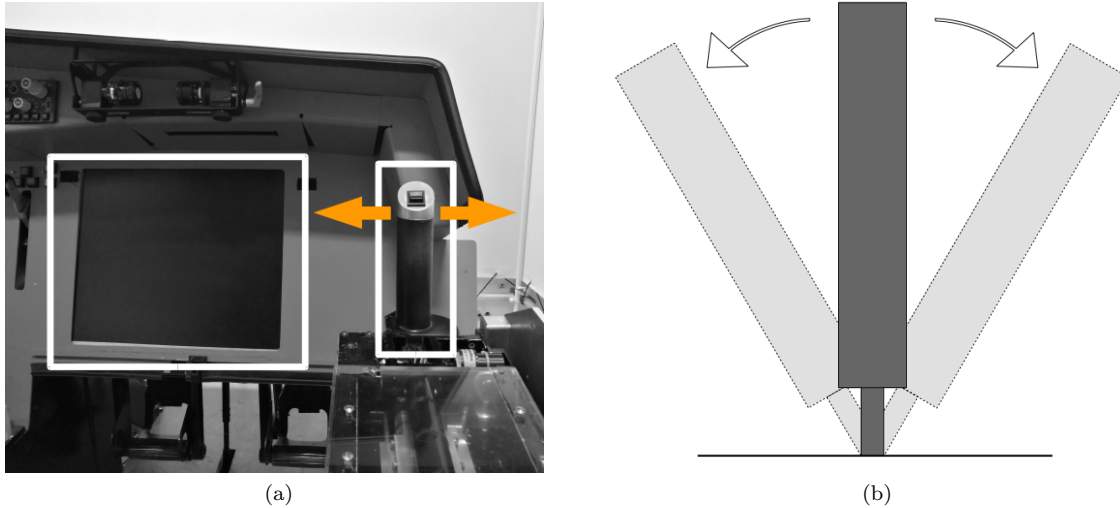
Figure 2: The devices used in the JND experiment. The sidestick and the LCD display are marked by white rectangles (a). The sidestick could be moved about the roll axis (left/right) like a joystick, as shown in (b).

Seven persons participated in the experiment. All participants were right-handed and reported no hand/arm impairment history. Experimental procedures and requirements were elaborated to participants, and an informed consent form was signed before the experiment.

III.B.   Conditions

A mass-spring-damping system was used in our work, whose dynamics are expressed as:

$$H(\omega) = m \cdot (j\omega)^2 + b \cdot (j\omega) + k \tag{4}$$

The setting of parameters of this system is given in Table 1. Note that we define units of parameters by the rotational convention, the force at grip can be obtained from the specification of the manipulator given in Section III.A. The frequency response of this system at the desired frequency of excitation (6 rad/s) is shown in Fig. 3, which gives identical projections on the two axes.

Four conditions are designed, we shall refer to the them as phase, imaginary, gain and real conditions respectively. In the phase condition, we shall examine the JND size in terms of changes only in the phase angle $\angle H$ (the magnitude $|H|$ does not change). In the gain condition, the JND for changes only in $|H(\omega)|$ is to be determined ($\angle H$ remained invariant). In the imaginary condition, the JND in terms of changes only in
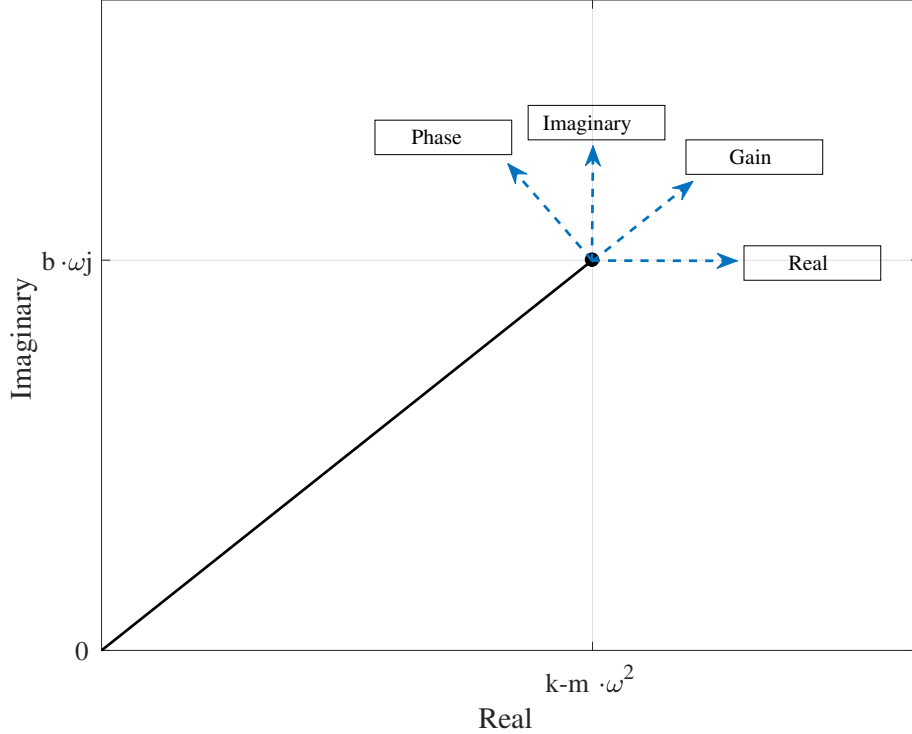
Figure 3: Illustrations of the reference system's frequency response and experimental conditions

the imaginary part P_{im} will be measured. In the real condition, the change only in P_{re} is considered. Note that we consider all changes as positive, respectively increments in the phase angle, the imaginary part, the magnitude and the real part, as shown by the arrows in Fig. 3.

III.C. Procedure

In this study, we normalize the size of changes in dynamics ($|\Delta H|$) to the magnitude of the frequency response of the reference system ($|H|$). Thus all JNDs could be measured as dimensionless fractions instead of complex numbers. The measurement of these JND fractions were achieved by an adaptive staircase procedure, as shown in Fig. 4.

A complete staircase procedure generally required 15-20 trials. In each trial, each subject was asked to identify the different one from three manipulator simulations. Thus there were three admissible answers, namely simulation 1, simulation 2 and simulation 3. Each simulation lasted 6.3 seconds. One of the three simulations was chosen randomly with a priori probability of 0.33 to simulate an adjustable setting of manipulator dynamics (the controlled setting H_c), and the rest two simulated a fixed setting (the reference dynamics H_r as defined in Table 1). The controlled setting H_c was defined as the reference dynamics plus an dynamic change in the direction defined by the testing condition ($H_c = H_r + \Delta H$). The size of ΔH was determined by the fraction being simulated in the current trial and the magnitude of the reference dynamics ($|\Delta H| = p \cdot |H_r|$). Each of the three simulations was first presented to subjects once. After that subjects could use the button on the side-stick to switch among simulations for re-comparisons as many times as the wished until they were willing to give the answer. The value of p for the next trial was reduced when a subject had correctly identified the simulation with the controlled setting, and was increased by a wrong identification. A reversal (shown by open circles in Fig. 4) is a point where the curve changes its direction. A procedure ends when the 7th reversal occurs, or the total trial number reaches 40. The average value of p in the last four reversal trials was taken as the measurement. Run time, indicating the starting and finishing time of each simulation, was shown on the LCD screen.

American Institute of Aeronautics and Astronautics
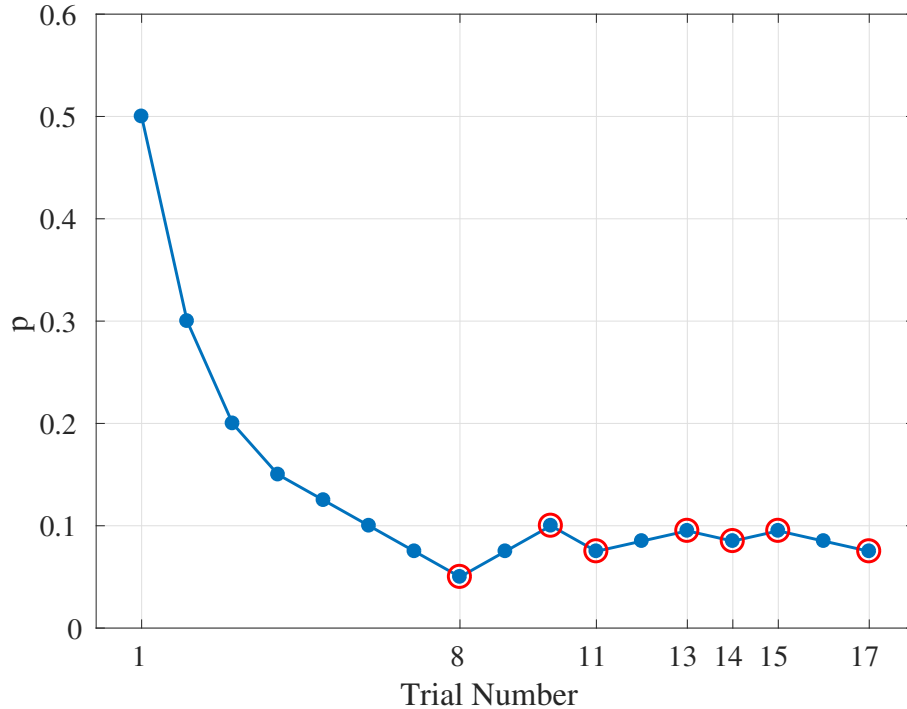
Figure 4: An example of the staircase procedure. Red circles represent reversals. p is adjusted by subjects' responses.

III.D. Visual display and side-stick motion control

In order to help subjects apply the desired manipulator motion, we asked them to perform a tracking task during each simulation. The visual display for the tracking task can be seen in Fig. 5. The frequency and amplitude of the reference manipulator angular displacement were 6 rad/s and 0.37 rad, respectively. A 1.5-second preview of the target angular displacement is shown as a winding curve moves downwards vertically across the display. The current target "+" is where the curve ends at the bottom (it only moves horizontally). The actual manipulator angular displacement is shown by an open circle (also only moves horizontally). Subjects were encouraged to reduce their tracking error $e(t)$ as possible as they could, and were given enough time to practice. 1-second fade-in and fade-out phases for eliminating possible transient responses are not shown in the figure.

IV. Results

Measurements of the JND fraction for different conditions are shown in Fig. 6. No significant effects of the direction of dynamic difference were indicated by the result from an one-way ANOVA ($F(3, 24) = 0.63$, $p = 0.6054$). The average fraction over all conditions was 7%.

Although similar JND sizes are found, the variation of individual observations for the phase condition is apparently larger than the other three conditions. One possible reason for this is that detecting a force difference caused by a phase shift is more difficult than others. This could be seen from the average number of re-comparisons per trial, as can be seen in Fig. 7. The average training time for the phase condition was also much longer than the other three conditions. Subjects generally asked for more time to familiarize themselves to the force change caused by a phase shift. We conjecture that this is because the lacking of experience with delayed forces.

Nevertheless, subjects still reached a similar level of sensitivity, implying that the raw noises in the force sensory process are the same for all these four cases. As for general cases symmetry of humans' haptic difference threshold exists. This means the lower JND could roughly be considered to be identical to the upper one. In our cases the JNDs in terms of decreases in $\angle H(\omega)$ (delay), $H(\omega)$, $P_{re}(\omega)$ and $P_{im}(\omega)$ should be

American Institute of Aeronautics and Astronautics
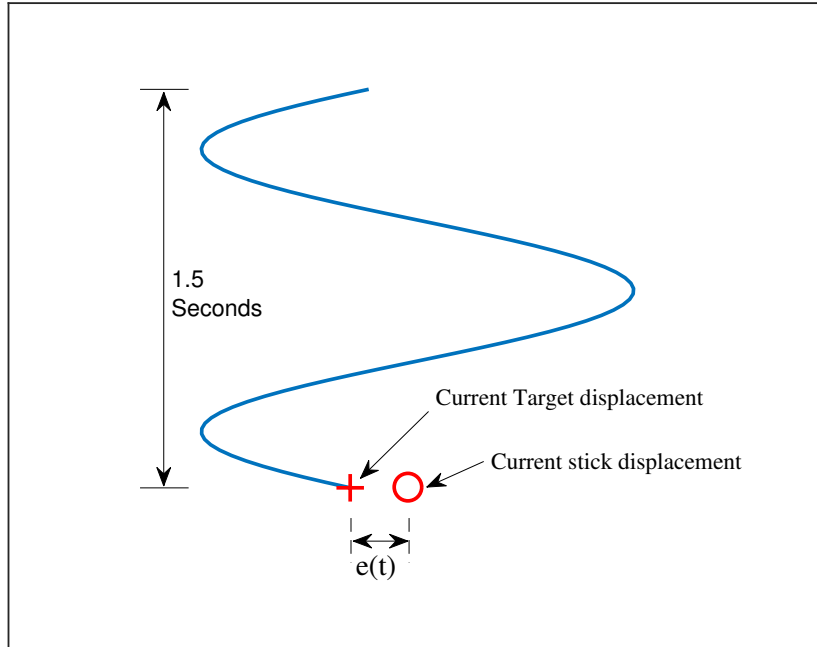
Figure 5: The visual display for the tracking task during each simulation.
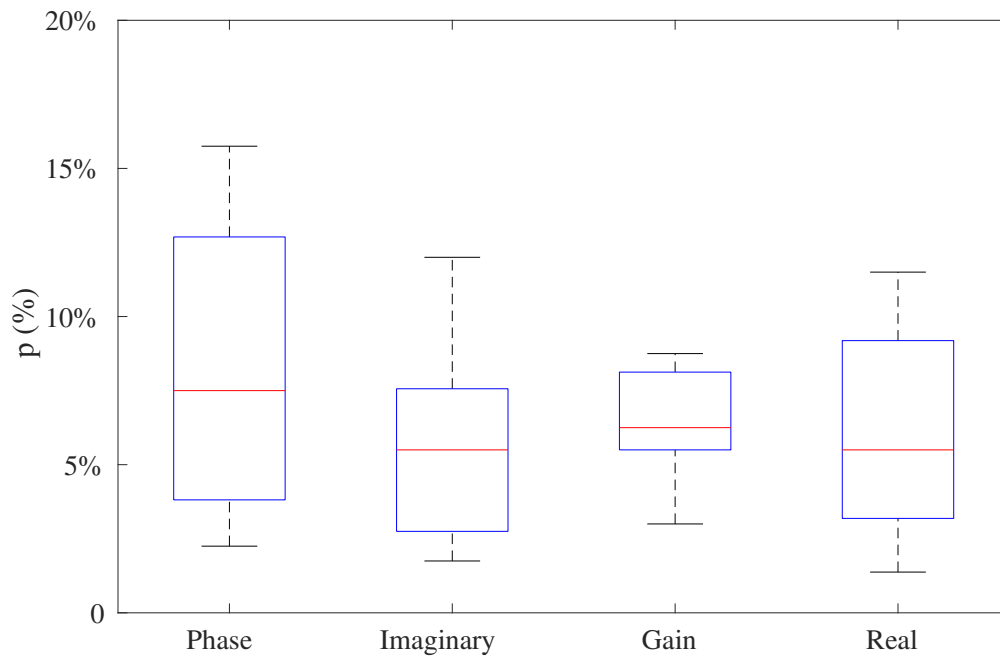
Figure 6: Boxplot of JND measurements.

similar to the results we obtained for incremental cases. With this consideration, changes with all directions could be roughly covered. Surprisingly, the JND in manipulator dynamics at 6 rad/s could be expressed in

American Institute of Aeronautics and Astronautics
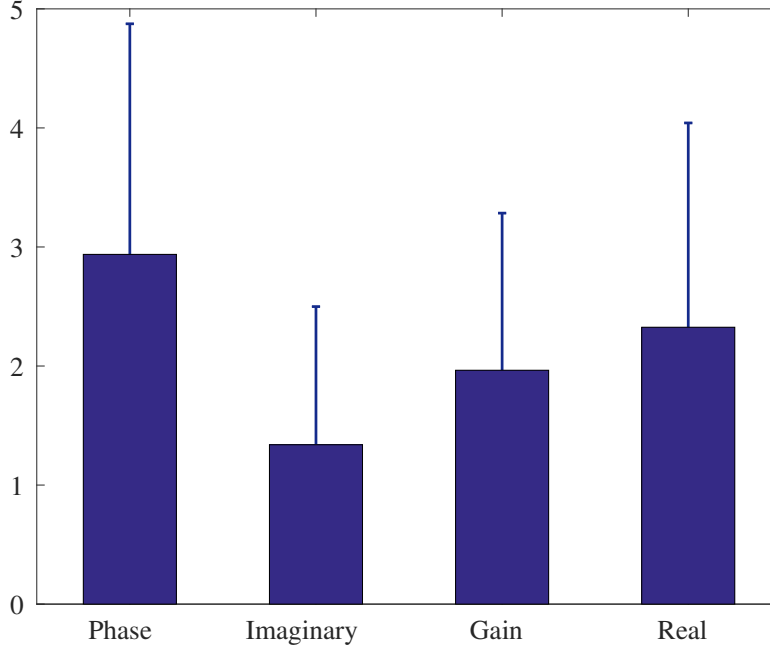
Figure 7: The average number over all subjects of re-comparisons per trial for conditions. Thin bars represent the standard deviations.

the way that the force JND is formulated (the Weber's law).

$$\frac{|\Delta H(\omega)|}{|H(\omega)|} = constant = 7\% \tag{5}$$

This equation formulates a circular area within which a change in dynamics should be unperceivable at this frequency, i.e., the perceptual fidelity region, as the shaded area shown in Fig. 8. This circular region allows us to determine if a simulated manipulator preserves the original feel, at 6 rad/s. If the dynamic vector of a simulated manipulator ends inside the circle, for example the system 1 expressed by the red dash line in Fig. 8, a human would perceive the same as the reference dynamics. Otherwise for example the blue dash line, a different feel would be rendered to the pilot.

V. OICT design

We have formulated the frequency-domain fidelity region for manipulator dynamics at 6 rad/s. We expect cases for other frequencies to be similar, as the principle of how humans discriminate between different sinusoidal forces should be independent of frequency. Since humans' active motion only covers a limited frequency range, we could assume the fraction p to be frequency independent. With this assumption, the JND in system dynamics can be defined as a function of the frequency. By defining $H_0(\omega)$ as the reference dynamics, we can define the boundary of the fidelity region $T(\omega)$ (the JND threshold) as:

$$T(\omega) = p \cdot |H_0(\omega)| \tag{6}$$

The evaluation of a manipulator simulation can be done at each individual frequency in a way similar to that shown in Fig. 8. This procedure can be simplified to comparing the radius of the circle $T(\omega)$ and the magnitude of the difference vector $|\Delta H(\omega)|$ at individual frequencies. In order to preserve the haptic feel of the reference dynamics during the simulation, the following inequality should be satisfied:

$$|\Delta H(\omega)| = |H_1(\omega) - H_0(\omega)| < p \cdot |H_0(\omega)| \tag{7}$$

American Institute of Aeronautics and Astronautics
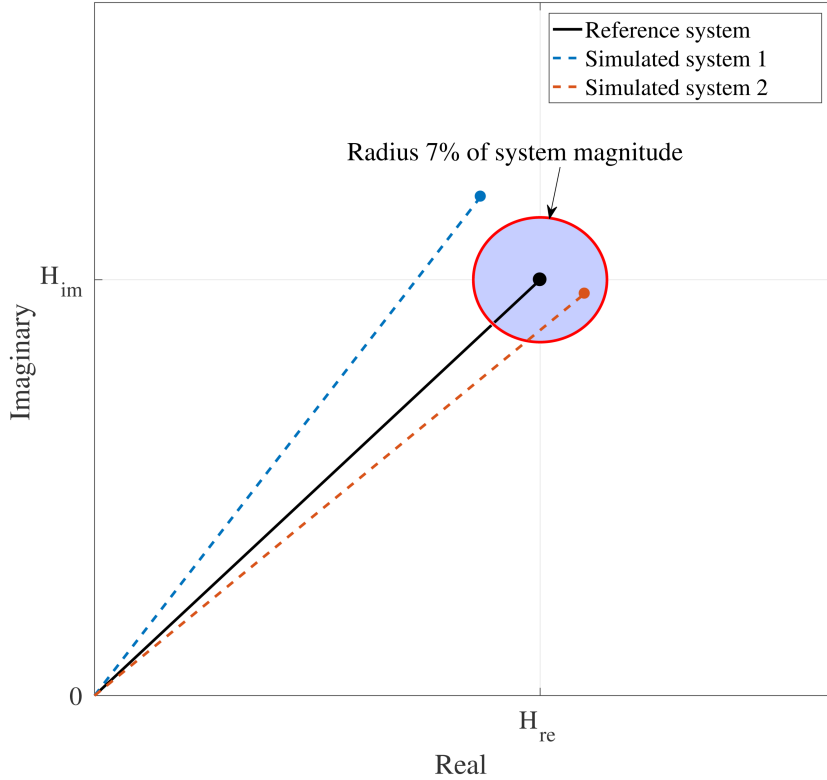
Figure 8: Frequency-domain haptic fidelity region for a specific frequency.

VI.   CLS Evaluation

For an illustration of what an OICT evaluation looks like, we shall evaluate our control loading device with a linear simulation. For our case, the reference model loaded in the control loading computer is defined by the admittance causality. With this definition, the system moves the control inceptor in response to the force measurements, as shown in Fig. 9.

The transfer function of the CLS can be expressed as:

$$D(\omega) = \frac{X}{F} = \frac{1}{H_1(\omega)} \quad , \tag{8}$$

in which H_1 is the transfer function defined by the position-force causality, which is required by the evaluation procedure. With the structure shown in Fig. 9, the simulated dynamics H_1 can be divided in two parts:

$$H_1(\omega) = H_0(\omega) \cdot H_d(\omega) \tag{9}$$

We use H_d to account for all the changes caused by the computation delay and dynamics of the control system. The first step of evaluation is of course to examine if the CLS is capable to ensure stability given the reference dynamics H_0. Here, assume H_0 is within the range of dynamics that ensure the stability of the whole system, the inequality in Eq. 7 can be simplified as:

$$|H_d(\omega) - 1| < p \tag{10}$$

This allows us to evaluate the control loading device independently of the reference dynamics. Once the device satisfies the above inequality, it can be used to simulate any allowable manipulator dynamics without rendering a different perception to the pilots. Due to this independence, examining the control loading device with one reference setting is representative.

American Institute of Aeronautics and Astronautics
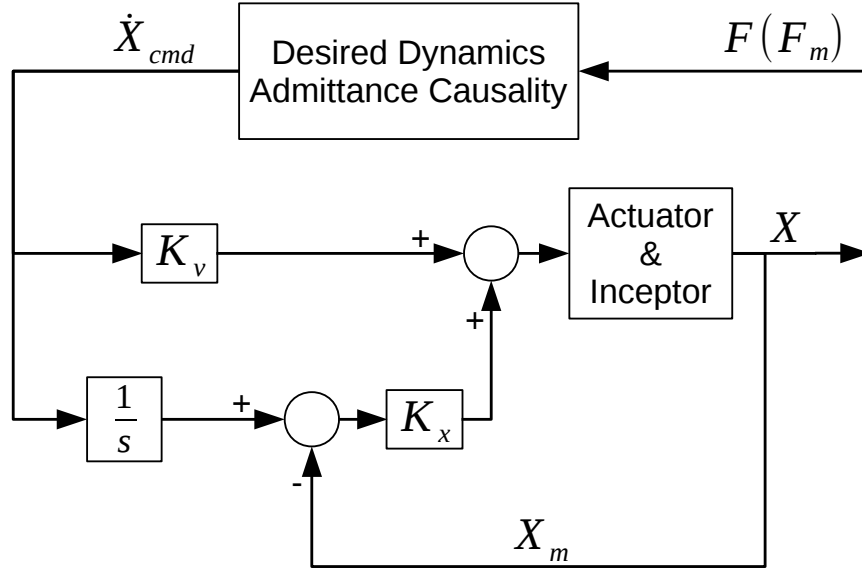
Figure 9: Structure of the control loading device.

We thus performed a linear side-stick simulation with the dynamics defined in Table 1, the same as the JND experiment. We estimated the frequency response of the control loading device $H_1(\omega)$ by the analysis of the power spectrum. A digital signal was used to represent the force measurement to feed the reference model in the control loading computer. This signal was defined by a multisine function with 25 elementary components in the frequency range from 0.05 rad/s to 20 rad/s. By selecting this range we could include the most possible excitation that a human operator could achieve. The quotient of the cross-spectral density function $\hat{S}_{fx}(\omega)$ and the auto-spectral density function $\hat{S}_{ff}$ would reflect how the inceptor moves in response to the force. Hence the dynamics of the simulated manipulator H_1 can be obtained by the reciprocal of this quotient:

$$\hat{H}_1(\omega) = \frac{1}{\hat{D}(\omega)} = \frac{\hat{S}_{ff}(\omega)}{\hat{S}_{fx}(\omega)} \tag{11}$$

The estimated dynamics of the simulated manipulator ($\hat{H}_1$) are shown with the reference dynamics (H_0) in the Nyquist plot for a comparison in Fig. 10. The difference between the desired and simulated dynamics increases with increasing frequency. This means the feel distortion becomes more evident when the control inceptor is moved faster. The fidelity regions at two frequency points, respectively A: 8 and B: 15.5 rad/s, are illustrated as examples as shown by the red circles. The black squares represent the frequency responses of the two systems at the corresponding frequencies. It can be seen that at 8 rad/s the difference between two systems is within the threshold circle, implying that a pilot would perceive these two system as the same when she/he moves the manipulator at this frequency. Whereas at 15.5 rad/s a different feel is presented by the manipulator simulation, since the end point of simulated dynamics is not enclosed by the threshold circle.

Since the input consists of 25 components, the CLS can be evaluated by Eq. 7 at 25 individual frequency points, as shown in Fig. 11. The two examples shown in Fig. 10 are marked by the black diamonds. The magnitude of the dynamic difference intersects the threshold at 11 rad/s, indicating that our device can preserve the original feel until the motion reaches 11 rad/s. As a common sense, a maneuver generally does not contain considerable energy above this frequency in its power spectrum. Our control loading device should be able to present the proper control feel for most flight tasks.

An advantage of our proposed approach is that the simulation fidelity of a CLS with the structure similar to that illustrated in this work could be evaluated independently of the reference dynamics once the reference dynamics are allowable for system stability. However, the implementation is limited only for linear cases. Since the stiffness property of most manipulators varies at different manipulator deflection ranges, we expect

American Institute of Aeronautics and Astronautics
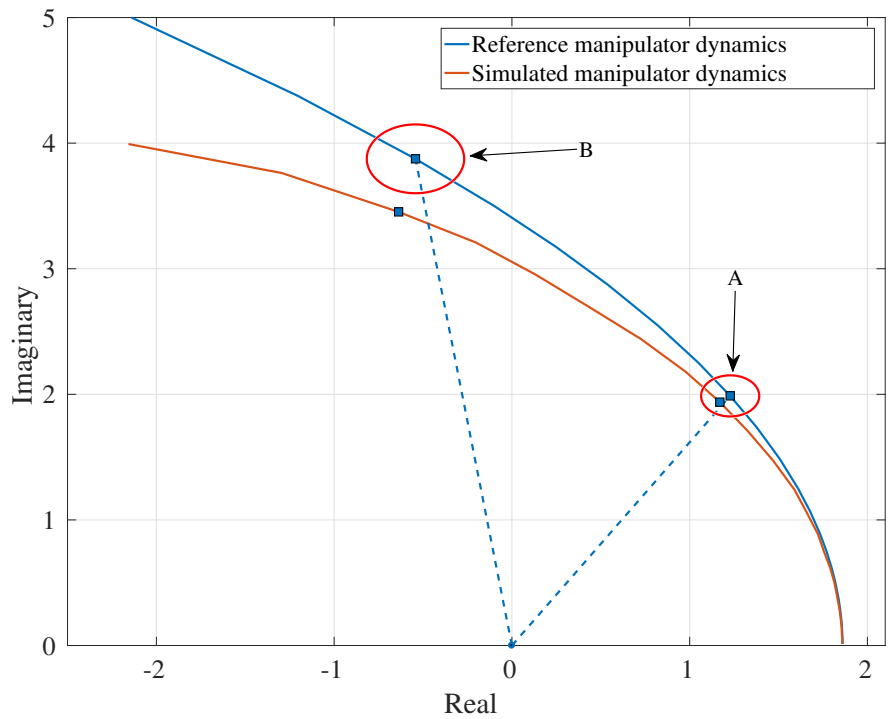
Figure 10: Reference and simulated manipulator dynamics.
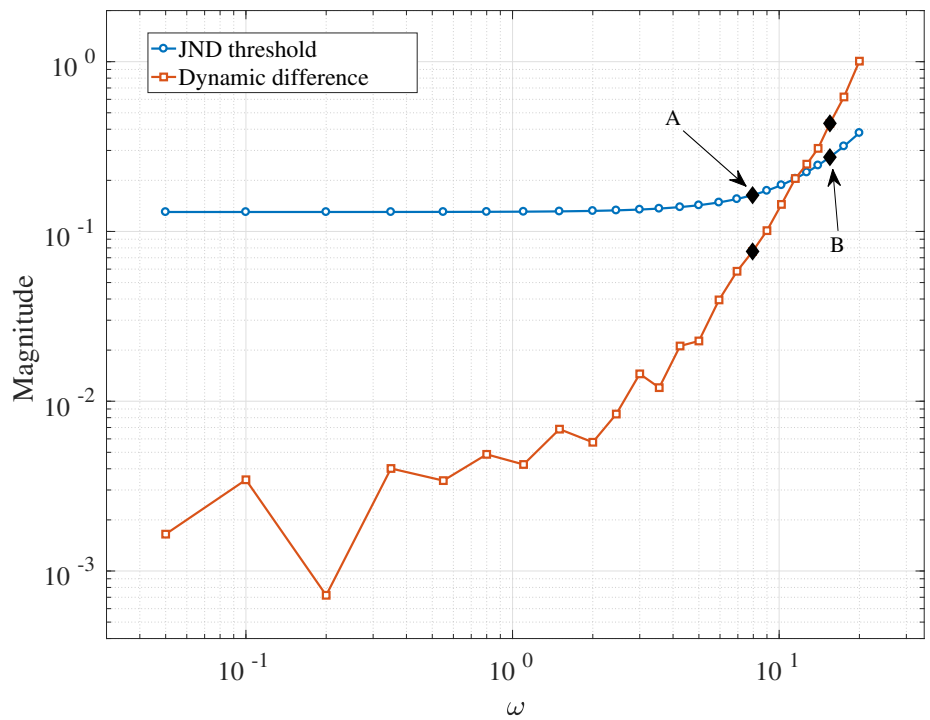
Figure 11: Comparison between the threshold and the dynamic difference.

to see whether this formulation also works for such nonlinear cases in further work.

The threshold fraction (7%) implemented in the evaluation was obtained when subjects were completely focusing on the dynamic discrimination, thus it represents a worst-case scenario. During a flight task, we expect a larger value since a pilot's attention is not on the dynamic comparison anymore. In addition, this fraction is currently measured on a side stick manipulator, moving which mainly requires excitation of muscles in the forearm. Cases for a central stick and a control column which involves more muscle groups such as those in the upper arm and the shoulder, the fraction may be slightly different. A more appropriate measurement taking account of these two factors need to be conducted in further work.

VII.   Conclusion

In this study, we presented a new evaluation design for control loading devices, namely the objective inceptor cueing test. In order to formulate the frequency-domain fidelity region for manipulator dynamics as a function of frequency, we consider the manipulator to be moved according to a sinusoidal motion. A experiment measuring the JNDs in terms of system frequency-response changes in phase angle, magnitude, real and imaginary parts was performed by seven human subjects. Results showed similar levels of JND for these four cases, and accordingly a JND model addressed in our previous work was extended to quantify the fidelity region. The frequency-domain tolerance for the control loading devices was then addressed. Our control loading device with an admittance control causality was evaluated as an example of the OICT design. Results showed that this device could simulate any allowable linear dynamics without changing the original control feel up to 11 rad/s.

Future work will be needed to determine the size of the JND at different frequencies of movement, and the JND for non-linear elements in the manipulator, such as friction, transitions in stiffness, break-out regions and end stops.

References

[1] Adams, R. and Hannaford, B., "Control law design for haptic interfaces to virtual reality," *IEEE Transactions on Control Systems Technology*, Vol. 10, No. 1, Jan. 2002, pp. 3–13.

[2] EASA, "CS-FSTD(A): Certification Specifications for Aeroplane Flight Simulation," Initial Issue, 2012.

[3] ICAO, "Manual of Criteria for the Qualification of Flight Simulation Training Devices," Doc 9625, 3rd edition, 2009.

[4] Van Paassen, M. M., Van Der Vaart, J. C., and Mulder, J. A., "Model of the Neuromuscular Dynamics of the Human Pilot's Arm," *Journal of Aircraft*, Vol. 41, No. 6, 2004, pp. 1482–1490.

[5] Jones, L. A., "Kinesthetic sensing," *Human and Machine Haptics*, MIT Press, 2000.

[6] Jones, L. A., "Matching forces: constant errors and differential thresholds," *Perception*, Vol. 18, No. 5, 1989, pp. 681–687.

[7] Pang, X. D., Tan, H. Z., and Durlach, N. I., "Manual Discrimination of Force Using Active Finger Motion," *Perception & Psychophysics*, Vol. 49, No. 6, 1991, pp. 531–540.

[8] Feyzabadi, S., Straube, S., Folgheraiter, M., Kirchner, E. A., Kim, S. K., and Albiez, J. C., "Human Force Discrimination During Active Arm Motion for Force Feedback Design," *IEEE Trans. Haptics*, Vol. 6, No. 3, 2013, pp. 309–319.

[9] Fu, W., van Paassen, M. M., and Mulder, M., "Modeling Haptic Masking for Mechanical Properties Discrimination from the Force Perception," *To be submitted*.